Int. J. Heat Mass Transfer. Vol. 19, pp. 431–441. Pergamon Press 1976. Printed in Great Britain

TURBULENT NATURAL CONVECTION OF LIQUID DEUTERIUM, HYDROGEN AND NITROGEN WITHIN ENCLOSED VESSELS*

DAVID E. DANEY
Cryogenics Division, Institute for Basic Standards, National Bureau of Standards, Boulder, CO 80302, U.S.A.

(*Received* 16 *July* 1975)

Abstract—Quasi-steady natural convection of liquid deuterium, hydrogen, and nitrogen within a sphere, hemisphere, horizontal cylinder, and vertical cylinder has been studied experimentally for the case of a nearly uniform wall temperature. A single expression relating the Nusselt and Rayleigh numbers,

$$Nu = 0{\cdot}104\,Ra^{0{\cdot}352},$$

fits the deuterium and nitrogen data over the range $7 \times 10^8 < Ra < 6 \times 10^{11}$, while the hydrogen Nusselt numbers are 8 per cent lower. The temperature field within the vessels is virtually free of horizontal temperature gradients. A single dimensionless temperature profile characterizes the vertical temperature distribution for each vessel shape, with the profiles for the sphere, hemisphere, and horizontal cylinder being nearly identical.

NOMENCLATURE

A, wall surface area;
C, modified specific heat, $= C_p + \beta(i_j - i)$;
C_1, proportionality constant in the Nusselt–Rayleigh number correlation defined by $Nu = C_1 Ra^n$;
C_2, proportionality constant;
C_p, specific heat at constant pressure;
D, diameter;
g, acceleration of gravity;
h, average heat-transfer coefficient;
i, specific enthalpy;
k, thermal conductivity;
L, cylinder length;
m, mass;
Nu, Nusselt number, $= \dfrac{hD}{k} = \dfrac{qD}{kA(T_b - \overline{T}_w)}$;
n, Rayleigh number exponent;
q, heat-transfer rate;
q_v, rate of internal heat generation per unit volume;
Ra, Rayleigh number, $= \dfrac{g\beta\rho^2 C_p D^3 (T_b - \overline{T}_w)}{\mu k}$
for vertical cylinders the characteristic length is L;
t, time;
T, absolute temperature;
T^*, dimensionless temperature, $= \dfrac{T - \overline{T}_w}{T_b - \overline{T}_w}$;
V, total volume;
v, specific volume;
w, velocity;
$\mathbf{W}$, velocity vector;
x, position.

Greek symbols

β, thermal expansivity, $= \dfrac{1}{v}\left(\dfrac{\partial v}{\partial T}\right)_p$;
μ, viscosity;
ρ, density;
σ, standard deviation.

Subscripts

b, bulk fluid;
c, core;
w, interior wall surface.

1. INTRODUCTION

NATURAL convection heat transfer within enclosures occurs in a number of applications. Cooling of turbine blades, heating and cooling of buildings and liquid storage tanks, cooling of nuclear fuel elements, and industrial process cooling are only a few examples. Cooling of liquid hydrogen and liquid deuterium moderators and targets for high energy physics experiments is another potentially useful application of natural convection heat transfer. This latter application has been used only at very low heating rates, however, because there is insufficient natural convection heat-transfer design information. In order to provide such information the experimental investigation reported here was undertaken.

Uniform internal heat generation which occurs within moderators and targets is difficult and expensive to achieve in heat-transfer experiments. Consequently, we simulated internal heat generation with a quasi-steady cooling process (i.e. cooling with a constant wall-to-fluid temperature difference).

The three parameters of primary interest in the design of these vessels are the average heat-transfer coefficient, the average bulk fluid temperature, and the maximum fluid temperature. The bulk temperature gives average fluid density and, hence, the mass of fluid within a vessel.

*Contribution of the National Bureau of Standards and not subject to copyright.

The maximum temperature gives the proximity to the boiling point, which in some applications is to be avoided. Also of considerable theoretical interest is the temperature field within a vessel because of the information it contains about the flow patterns. In this study the average heat-transfer coefficient and the temperature field were determined for turbulent natural convection heat transfer with liquid deuterium (LD_2), liquid hydrogen (LH_2), and liquid nitrogen (LN_2) enclosed within spheres, hemispheres, horizontal cylinders, and vertical cylinders with nearly uniform wall temperature. Quasi-steady cooling was the primary mode studied, although results are also given for quasi-steady heating and transient cooling. The Rayleigh numbers ranged from 7×10^8 to 6×10^{11} and the temperatures range from 20 K to 26 K for LH_2 and LD_2 and 78 to 88 K for LN_2.

The previous experimental studies of natural convection within enclosures have been concerned with either laminar convection or with transient convection. None of these investigated quasi-steady turbulent flow or used cryogenic fluids, and most are confined to laminar convective flow. Schmidt [1] gives *Nu* vs *Ra* and some temperature profile data for transient turbulent free convection in spheres up to 50 cm in diameter using water and various alcohols. Evans and Stefany [2], and Maahs [3] investigated transient laminar free convection in horizontal cylinders using water, *n*-butanol, methanol and water–glycerine mixtures. Deaver and Eckert [4] studied quasi-steady laminar free convection within horizontal cylinders using water and ethylene glycol. A considerable effort, both analytical and experimental, has been spent on transient free convection in vertical cylinders and on the associated thermal stratification. Clark [5] has summarized this work; and some of the more relevant experimental studies are by Evans and Stefany [2], Evans, Reid and Drake [6], Schwind and Vliet [7], Tatom and Carlson [8] and Barakat and Clark [9].

ANALYSIS

The analogy between quasi-steady cooling and uniform internal heat generation results because of the similar effects on the convection process caused by the fluid heat capacity and by uniform internal heat generation. Inspection of the energy equation shows this analogy is exact. For a low Mach number, constant pressure, and constant thermal conductivity system, the energy equation is

$$\rho C_p\left[\frac{\partial T}{\partial t}+\mathbf{W}.\nabla T\right]=k\nabla^2 T+q_v. \tag{1}$$

Rearranging equation (1) so that the terms defining the velocity and temperature field are on the right hand side gives

$$\rho C_p\frac{\partial T}{\partial t}-q_v=k\nabla^2 T-\rho C_p\mathbf{W}.\nabla T. \tag{2}$$

The individual contributions that the terms on the L.H.S. of equation (2) make to the velocity and temperature fields are indistinguishable since the variables are separable in this fashion. Thus, the velocity and temperature fields within a vessel for the constant rate of cooling case,

$$\rho C_p\frac{\partial T}{\partial t}=\text{constant} \tag{3}$$

and

$$q_v=0, \tag{4}$$

should be the same as for the steady state uniform internal heating case,

$$q_v=\text{constant} \tag{5}$$

and

$$\rho C_p\frac{\partial T}{\partial t}=0. \tag{6}$$

More formally, by transforming equation (2) using $\varphi = T-\overline{T}_w$, the requirements for quasi-steady cooling are:

$$\rho C_p\frac{\partial \overline{T}_w}{\partial t}=\text{constant} \tag{7}$$

and

$$T-\overline{T}_w=\text{constant}. \tag{8}$$

In controlling the experimental conditions the latter criterion was used, whereas in the selection of the data to be analyzed, both criteria were used.

In selecting correlating parameters, we assumed that steady-state parameters are also valid for quasi-steady conditions—an assumption that is supported by these experimental results. Thus we use the expression

$$Nu=C_1 Ra^n \tag{9}$$

to correlate the heat-transfer coefficient data. The characteristic temperature difference used in the Nusselt number and Rayleigh number is $T_b-\overline{T}_w$, and the fluid properties were evaluated at the bulk fluid temperature T_b. We use the surface average heat-transfer coefficient, so that the Nusselt number is given by

$$Nu=\frac{\bar{h}D}{k}=\frac{(\bar{q}/A)D}{(T_b-\overline{T}_w)k}. \tag{10}$$

The characteristic length is the vessel diameter for the sphere, hemispheres, and horizontal cylinder; and the height for the vertical cylinders.

The temperature profile data were correlated using the dimensionless temperature

$$T^*=\frac{T-\overline{T}_w}{T_b-\overline{T}_w}, \tag{11}$$

which is simply the local temperature difference, $T-\overline{T}_w$, normalized by the characteristic temperature difference, $T_b-\overline{T}_w$.

The parameter T^* yields a single dimensionless temperature profile for each shape when the flow is fully developed, because identical T^* profiles imply similitude of velocity fields. This connection between the velocity and temperature fields is most easily visualized by considering the uniform internal heat generation

case. If we follow a fluid element rising within the vessel, then (in the absence of heat transfer or mixing), the temperature rise of that element is proportional to the time of travel from our datum point, and the slope of the temperature, dT/dx, is inversely proportional to the velocity. Changing the heating rate or the magnitude of the velocity will change the temperature difference at a given point within the vessel, but it will not change the temperature difference relative to the volume average (bulk) temperature difference within the vessel.

From the definition of T^*, we find that at the wall

$$T_w^* \equiv 0, \tag{12}$$

and for the bulk fluid

$$T_b^* \equiv 1. \tag{13}$$

We obtain the actual temperature at any point within a vessel using the identity

$$T - \bar{T}_w \equiv T^*(T_b - \bar{T}_w), \tag{14}$$

where $T - \bar{T}_w$ is obtained from the Nusselt–Rayleigh number correlation.

EXPERIMENTAL

Figure 1 is a schematic of the experimental apparatus. The different test fluids used in the experimental vessels required different bath fluids: a liquid hydrogen bath for the liquid deuterium and hydrogen tests, and a liquid nitrogen bath for the liquid nitrogen tests. Consider a liquid hydrogen experiment. The hydrogen bath is warmed to about 28 K by bubbling warm hydrogen gas through the liquid and pressurizing the dewar to about 7·5 atm. After the fluid in the test vessel has come to within 0·5 K or less of the bath temperature, the valve to the vent line is cracked, and the temperature of the bath falls as the bath pressure is bled down to atmospheric pressure or below. During the process a constant temperature difference is maintained between the fluid in the test vessel and the vessel wall by observing the signal from one of the differential thermocouples and adjusting the valve-opening accordingly. If the fluid properties were independent of temperature, cooling with a constant rate of heat removal would result. In practice, however, variation of the thermal properties with temperature results in a slowly decreasing heat-transfer rate.

During the cooling (or heating) process, temperatures within the test vessel, and at the test vessel wall were measured with differential thermocouples referenced to the bath temperature, and the absolute temperature of the bath was measured with a fast response platinum resistance thermometer. From these measured temperatures the quantities of interest may be calculated: $\bar{T}_w$, $T_{\text{fluid}} - \bar{T}_w$, $T_b - \bar{T}_w$, and $\partial T_b/\partial t$ (which gives q). The bulk temperature, T_b, and the average wall temperature $\bar{T}_w$ are obtained from weighted averages of the fluid and wall temperature measurements.

Most of the data were collected during the cooldown mode of operation. The constant-temperature-difference operation was easier to achieve in this mode, and the bath temperature was uniform providing a good reference temperature for the thermocouples. Data were also collected during warm-up, although the experiment was more difficult to control, and the accuracy was lower.

The design of the test vessels (Fig. 2 shows a typical example) was governed largely by the test environment of differential pressures up to 3·4 atm in either direction, and temperatures down to 15 K. Nearly adiabatic walls were provided by high density (0·1 g/cm^3 to prevent crushing by the pressure) styrofoam or glass reinforced epoxy. Because of the high coefficient of thermal expansion of liquid hydrogen and liquid deuterium (about 2%/°K), a liquid ballast volume must be connected to the test vessel to assure that the vessel remains full at all times. To prevent boiling or vapor formation in the test vessel, the surface of the liquid in this ballast volume is pressurized to about 4 atm with helium gas. No evidence of helium gas desorption in the test vessel was observed.

In order to study the effects of the wall resistances on the convection process, three hemispheres with different wall resistances were tested. Table 1 summarizes the geometries and characteristics of the experimental vessels. The ends of both the vertical and horizontal cylinders are insulated.

Instrumentation

Chromel vs gold (0·07 atomic percent iron) differential thermocouples were chosen to measure the enclosed fluid and vessel wall temperatures because of the high sensitivity these thermocouples exhibit at liquid hydrogen temperatures (approximately 16 μV/K). The wire

Table 1. Test vessel characteristics

Shape	Wall materials	D (cm)	L/D	V (l)	A (cm^3)	Wall plus outside film resistance (cm^2.K/W)
Sphere	Copper	9·8		0·521	318·0	3·9
Hemisphere	Copper	6·5		0·072	66·3	3·9
Hemisphere	Copper	17·1		1·228	438·2	3·9
Hemisphere	Stainless steel	17·1		1·198	433·4	7·7
Hemisphere	Plastic–copper laminate	17·1		1·220	436·3	10·0
Horizontal cylinder	Copper (ends insulated)	7·4	4	1·274	687·6	3·9
Vertical cylinder	Copper (ends insulated)	7·4	4	1·274	687·6	3·9
Vertical cylinder	Copper (ends insulated)	7·4	2	0·637	343·8	3·9

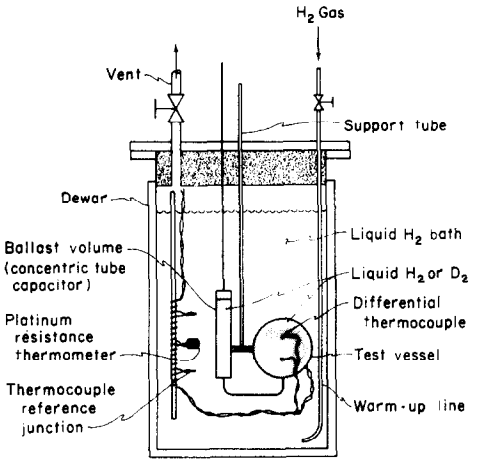

FIG. 1. Experimental apparatus.

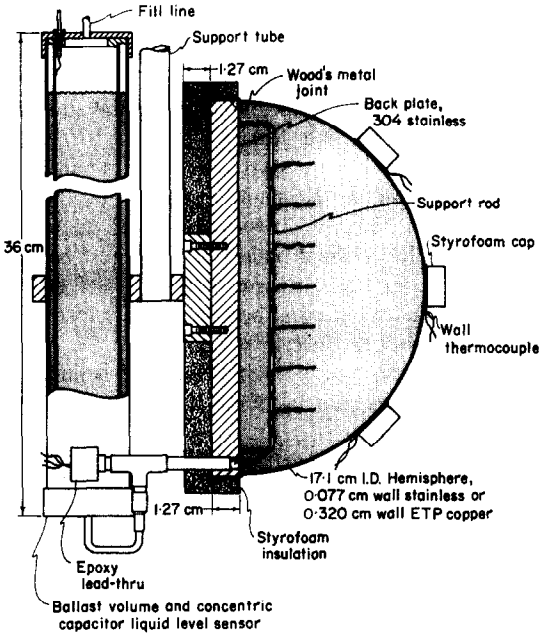

FIG. 2. Test vessel—17·1 cm dia hemisphere.

diameters are 0·15 mm for the gold–iron and 0·22 mm for the chromel, and the reference junctions lie in the liquid bath as illustrated in Fig. 1. Thermal tempering of the thermocouples within the test vessels was accomplished by simply cantilevering the wires horizontally for about 4 cm from their support rod as shown in Fig. 2. The fluid thermocouples are generally aligned on the vertical axis in the sphere, vertical cylinders, and horizontal cylinders; and aligned along a vertical line displaced from the back plate, 1·0 cm for the 17·1-cm dia hemispheres, and 0·5 cm for the 6·5-cm dia hemisphere. In a few tests some of the thermocouple junctions were distributed horizontally in an attempt to measure horizontal temperature gradients.

The wall temperature was measured by mounting the thermocouples on the exterior surface of the wall as illustrated in Fig. 3. This technique is suitable only for walls with a high thermal conductance if the wall

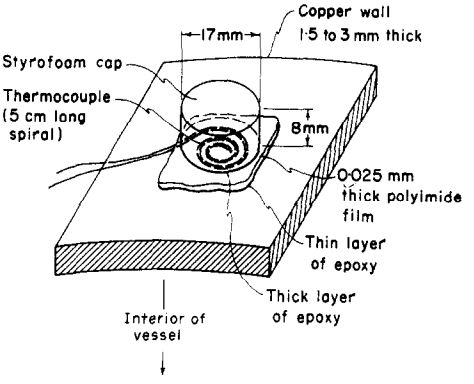

FIG. 3. Wall thermocouple installation—copper walls.

temperature drop from the edge to the center of the cap is to be kept small. Thus the inside wall temperature for the stainless steel and copper–plastic walled vessels was obtained using the outside film resistance measured for the copper vessels together with a calculated wall resistance.

In assessing the experimental error, the agreement between thermocouples was generally better than 0·05 K, and the estimated systematic error was 3 per cent or less of $T-\bar{T}_w$. The systematic error in the heat flux is estimated to be less than 10 per cent for the insulated wall vessels (all vessels except the sphere) and about 5 per cent for the sphere. The overall systematic error of the correlations is estimated to be less than 13 per cent for all of the fluids used in this study. In applying the correlations to other fluids, an additional systematic error of 10 per cent could be present because of the uncertainty in the thermal properties (principally the thermal conductivity) of liquid deuterium. The random error in Nusselt number for the overall correlation is typified by a standard deviation of 10 per cent.

Data reduction

Data reduction is a two-step process. First, the e.m.f.s, which are recorded on magnetic tape by a data logger, are converted to temperatures and heating rates by a digital computer. Then, these temperature and heating rate data are scanned by eye, and points sufficiently quasi-steady in nature are selected for evaluation of the Nusselt number, Rayleigh number, and dimensionless temperature profile. The criteria for quasi-steady state were generally that T_b-T_w should not vary by more than plus or minus 2 per cent, and that q should not vary by more than about 10 per cent over a 30 s interval.

The bulk temperature of the fluid is calculated from a weighted average of the interior thermocouple readings. Weights are assigned as the fraction of the total volume occupied by a horizontal segment having the thermocouple located at its vertical center. An absence of horizontal temperature gradients in the bulk of the fluid makes this the appropriate method of weighting. The boundary layer is neglected in this calculation, but its contribution should be small, since attempts to directly measure the inside wall temperature indicated that the boundary layer is only a fraction of a millimeter thick.

The average wall temperature is calculated from a weighted average in a manner similar to the bulk temperature calculation. Weights are assigned according to the fraction of the total wall surface area between horizontal planes equidistant from the thermocouples. Because the inside wall temperature of the stainless steel and the plastic–copper hemispheres could not be measured, these wall temperatures were calculated using the wall and film resistances given in Table 1.

The heat transferred is determined from the time rate of change of the bulk temperature according to the expression

$$q = \rho V C \frac{\partial T_b}{\partial t}. \tag{15}$$

For warm-up type experiments, in which fluid is expelled from the vessel, C is simply the specific heat at constant pressure, C_p. For cool-down experiments, however, allowance must be made for fluid entering the vessel cooler than the fluid within the vessel. In this case,

$$C = C_p + \beta(i_j - i) \tag{16}$$

where i_j is the specific enthalpy of the fluid entering the vessel, and i is the specific enthalpy of the fluid within the vessel [10].

THERMAL PROPERTIES

Table 2 lists the thermal properties of the test fluids as a function of temperature. Because of the large relative span in absolute temperature covered by deuterium and hydrogen, the properties of these two fluids exhibit a particularly strong temperature dependence.

Table 2. Thermal properties of the test fluids at 4 atm

T (K)	β (1/K)	ρ (mol/cm^3)	Cp (J/mol.K)	μ (g/cm.s)	k (W/cm.K)	$g\beta\rho^2 Cp/\mu k$ (1/cm^3.K)	Pr
			Liquid deuterium				
20	0·0120	0·0427	22·8	368×10^{-6}	$1{\cdot}01 \times 10^{-3}$	$5{\cdot}28 \times 10^{6}$	2·06
22	0·0136	0·0416	24·8	318	1·04	6·95	1·88
24	0·0156	0·0404	27·0	276	1·08	9·14	1·71
26	0·0182	0·0390	29·6	246	1·11	11·91	1·63
28	0·0220	0·0375	32·8	221	1·11	16·30	1·62
Ref.	[11]	[11]	[12, 13]	[14]	[15]		
Estimated Uncertainty	2%	0·5%	1%	2%	20%	25%	24%
			Liquid hydrogen				
16	0·0117	0·0375	14·8	201×10^{-6}	$0{\cdot}90 \times 10^{-3}$	$2{\cdot}67 \times 10^{6}$	1·64
18	0·0134	0·0366	16·7	164	0·97	3·73	1·40
20	0·0154	0·0355	18·8	139	1·00	5·21	1·30
22	0·0184	0·0344	21·4	118	1·02	7·59	1·23
24	0·0228	0·0330	24·6	103	1·02	11·49	1·23
Ref.	[16]	[16]	[16]	[17]	[17]		
Estimated Uncertainty	1%	0·1%	0·5%	0·5%	3%	5%	4%
			Liquid nitrogen				
74	0·0053	0·0294	57·7	173×10^{-5}	$1{\cdot}38 \times 10^{-3}$	$3{\cdot}04 \times 10^{6}$	2·58
76	0·0055	0·0291	57·6	160	1·36	3·38	2·41
78	0·0057	0·0287	57·5	148	1·33	3·78	2·28
80	0·0059	0·0284	57·5	138	1·30	4·21	2·18
82	0·0062	0·0281	57·5	129	1·27	4·67	2·09
84	0·0064	0·0277	57·6	120	1·24	5·23	1·99
86	0·0067	0·0274	57·9	113	1·21	5·80	1·93
Ref.	[18]	[18]	[18]	[19]	[19]		
Estimated Uncertainty	2%	0·5%	2%	2%	4%	10%	8%

A large uncertainty is assigned to the thermal conductivity of liquid deuterium because of the discrepancy (20 per cent) between the conductivity values given by Powers *et al.* [20] and Roder and Diller [21] for liquid hydrogen. The Roder and Diller values for hydrogen are taken as correct in this paper, and since Powers *et al.* used the same apparatus for LD_2 and LH_2, the Powers values for LD_2 have been reduced by 20 per cent. In spite of this correction, a 20 per cent uncertainty is possible in the LD_2 thermal conductivity. However, intercomparison of the LH_2 and LD_2 Nusselt numbers indicates that this uncertainty may be closer to 10 per cent.

RESULTS AND DISCUSSION

Figures 4–6 summarize the cooling results for the copper walled vessels. The curves for Nu were obtained from a least squares curve fit to the expression $Nu = C_1 Ra^n$. Only the liquid deuterium and liquid nitrogen data were used to obtain the expressions and curves shown in the figures because the hydrogen data

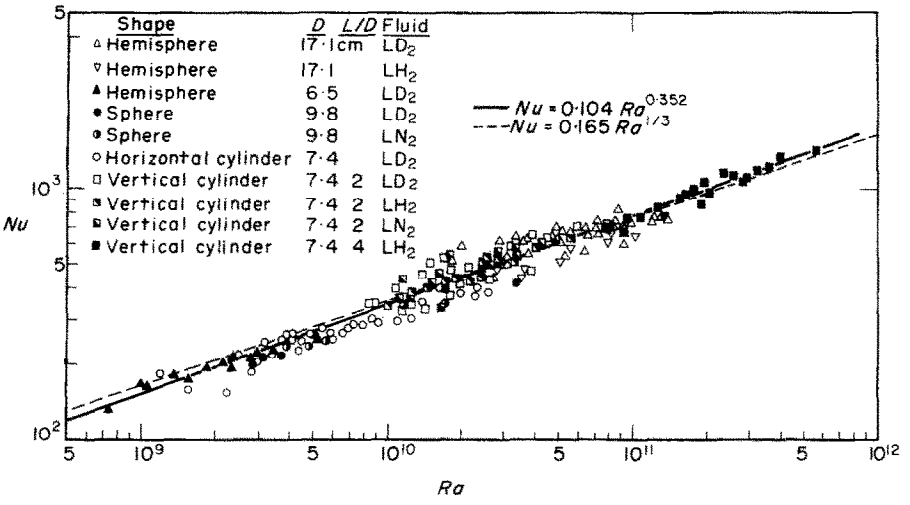

FIG. 4. Summary of Nusselt number data for all cooling experiments in copper walled vessels. The correlations and curves are for the LD_2 data only.

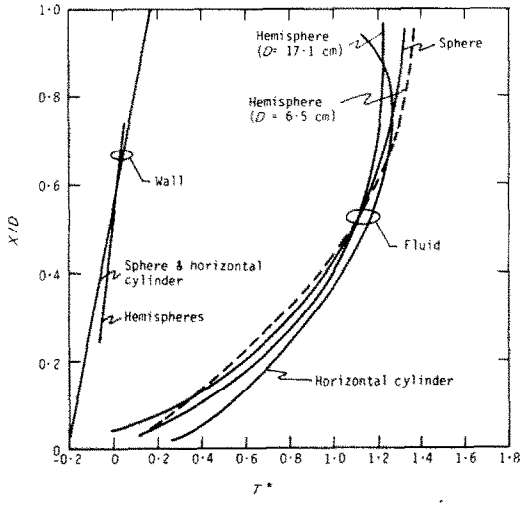

FIG. 5. Vertical temperature distributions of the copper walled hemispheres, sphere, and horizontal cylinder for the cooling experiments. The fluid is liquid deuterium.

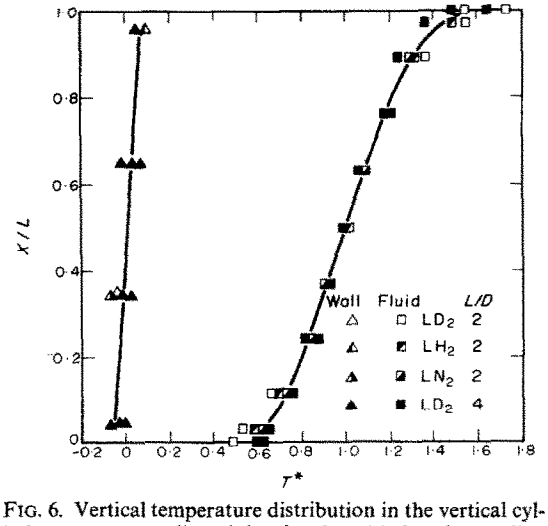

FIG. 6. Vertical temperature distribution in the vertical cylinders (copper wall and insulated ends) for the cooling experiments.

have a mean negative deviation of 8·4 per cent from the deuterium and nitrogen data. This discrepancy is probably due to the uncertainty in the thermal properties, although it should be noted that the Prandtl number of LH_2 is about 50 per cent lower than that of LD_2 or LN_2. A summary of the curve fits and the resulting standard deviations for the individual shapes is given in Table 3.

Use of the dimensionless temperature,

$$T^* = \frac{T - \bar{T}_w}{T_b - \bar{T}_w},$$

results in a single dimensionless temperature profile for each shape when the flow is fully developed. Because of the virtual absence of horizontal temperature gradients within the vessels (except in the boundary layer), the temperature in any given horizontal plane is characterized by a single temperature. The standard deviation of T^* is about 0·03 at most points within the vessels. At the top of the vertical cylinders, σ of T^* is as large as 0·08.

Figure 7 gives the Nusselt number data for the warming experiments. Although of lower accuracy than the cooling data, these results demonstrate that, as expected, the Nusselt numbers are essentially the same for heating and cooling. The 7·2 per cent systematic difference between the heating and cooling data is within the experimental error. Figures 8 and 9 show temperature profiles measured during warming. The generally larger wall temperature gradients (comparing Fig. 6 with Fig. 9) result because of the lower outside wall heat-transfer coefficients experienced during warming.

Following the quasi-steady cooling period, transient cooling of the vessels occurred with a nearly constant bath temperature. Figure 10 compares a typical cooling curve with calculated cooling curves based on the quasi-steady cooling correlations. The solid curve assumes the heat-transfer coefficient depends on the instantaneous value of $T_b - \bar{T}_w$, whereas the dashed curve

Table 3. Correlation results using the expression $Nu = C_1 Ra^n$

Test vessel	Fluid	C_1	n	Std. Dev. (%) in Nu
Sphere (copper)	LD_2	0·446	0·284	4·2
D = 9·8 cm		0·974	1/4	5·0
		0·140	1/3	5·9
Sphere (copper)	LN_2	0·162	0·327	7·0
D = 9·8 cm		0·140	1/3	7·0
Copper hemisphere	LD_2	0·470	0·281	3·0
D = 6·5 cm		0·935	1/4	3·6
		0·150	1/3	
Copper hemisphere	LD_2	5·19	0·195	8·6
D = 17·1 cm		1·32	1/4	9·1
		0·164	1/3	11·1
Copper hemisphere	LH_2	0·197	0·321	5·2
D = 17·1 cm		1·16	1/4	6·0
		0·147	1/3	5·2
Stainless steel hemisphere	LD_2	0·349	0·297	10·2
D = 17·1 cm		0·141	1/3	10·4
Plastic–copper hemisphere	LD_2	5·03	0·191	5·6
D = 17·1 cm		1·17	1/4	6·3
		0·150	1/3	8·9
Horizontal cylinder (copper)	LD_2	0·259	0·309	7·8
D = 7·4 cm		0·151	1/3	8·0
Vertical cylinder (copper)	LD_2	0·109	0·352	10·8
D = 7·4 cm, L/D = 2		0·171	1/3	10·8
Vertical cylinder (copper)	LH_2	0·00554	0·379	4·0
D = 7·4 cm, L/D = 2		0·163	1/3	4·3
Vertical cylinder (copper)	LN_2	0·212	0·324	7·2
D = 7·4 cm, L/D = 2		0·170	1/3	7·2
Vertical cylinder (copper)	LD_2	$4{\cdot}51(10)^{-3}$	0·483	5·0
with heater, D = 7·4 cm, L/D = 2		1·62	1/3	8·6
Vertical cylinder (copper)	LD_2	0·0720	0·366	5·2
D = 7·4 cm, L/D = 4		0·170	1/3	5·5
Sphere (copper)	LD_2 & LN_2	0·376	0·291	5·4
D = 9·8 cm		0·140	1/3	6·3
Copper hemispheres	LD_2	0·263	0·314	16·6
D = 6·5 cm, 17·1 cm		0·164	1/3	16·9
Vertical cylinders	LD_2	0·152	0·338	7·8
D = 7·4 cm, L/D = 2·4		0·171	1/3	7·8
All copper vessels	LD_2	0·104	0·352	10·7
cooling		0·166	1/3	11·0
All copper vessels	All	0·939	0·356	10·4
cooling	fluids	0·165	1/3	10·6
All copper vessels	LD_2	0·104	0·355	17·1
warming		0·177	1/3	17·9

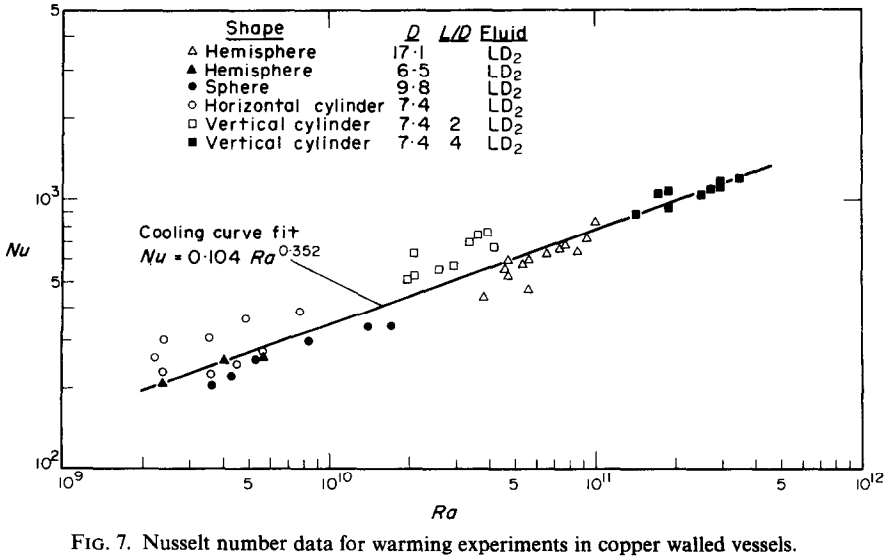

FIG. 7. Nusselt number data for warming experiments in copper walled vessels.

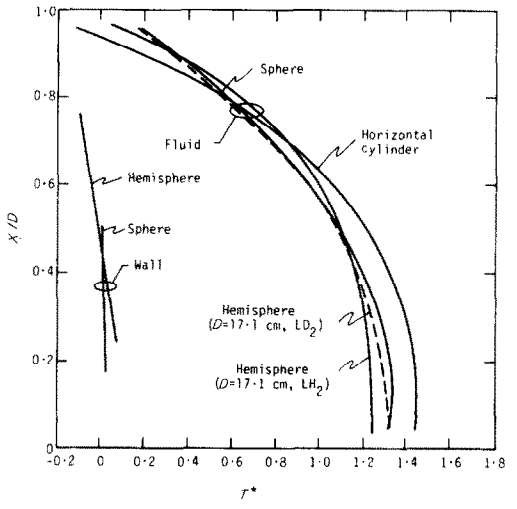

FIG. 8. Vertical temperature distributions of the hemisphere, sphere, and horizontal cylinder for the warming experiments. Unless specified, the fluid is liquid deuterium.

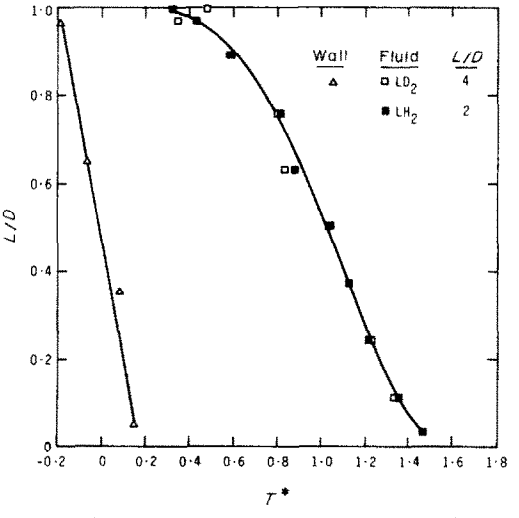

FIG. 9. Vertical temperature distribution in the vertical cylinders (copper wall and insulated ends) for the warming experiments.

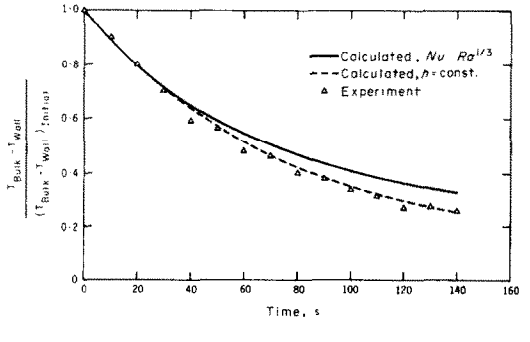

FIG. 10. Transient response of LD_2 within a copper sphere.

assumes a constant heat-transfer coefficient that is evaluated using $(T_b - \overline{T}_w)_{\text{initial}}$. Agreement of the constant h curve with the experimental data is in accord with the results of Evans and Stefany [2], who observed constant h cooling in their transient experiments.

Temperature profiles

The temperature field within a vessel provides considerable information about the convective process. The virtual absence of horizontal temperature gradients, and a thin boundary-layer thickness are characteristic of all the vessels. The virtual absence of horizontal temperature gradients is illustrated in Fig. 11, which is a composite of the temperatures measured in several different hemisphere experiments. Measurements in other vessels gave similar results.

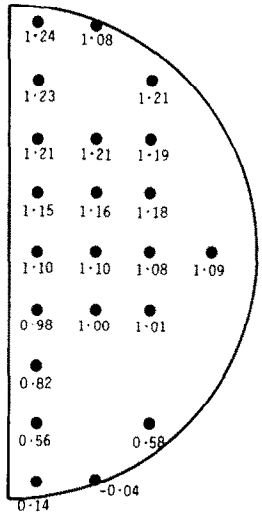

FIG. 11. Dimensionless temperature, T^*, within 17·1 cm dia hemisphere for cooling experiments. Measurements are in the vertical plane bisecting the hemisphere.

We obtained information on the boundary-layer thickness while attempting to measure the inside wall temperature directly. Thermocouples 0·1-mm thick were glued to the inside wall of the stainless steel hemisphere. These thermocouples measured temperatures about midway between the fluid temperature and the calculated wall temperature, indicating a boundary-layer thickness of only a few tenths of a millimeter. This thickness agrees with the value of 1-mm or less observed by Evans *et al.* [6].

The temperature profiles for the sphere, hemisphere, and horizontal cylinder (Fig. 5) are quite similar, indicating a common flow pattern for all three shapes. The relatively small vertical temperature gradient in the upper portion of these vessels for the cooling experiments (lower portion of the vessel for heating experiments) indicates highly turbulent mixing in this region. Schmidt [1] observed this condition in Schlieren photographs of free convection within a horizontal cylinder. The temperature gradient for cooling in the lower portion of the sphere, hemispheres, and horizontal cylinder indicates that boundary-layer fluid enters the core all along this region. This conclusion becomes apparent if we consider the uniform heat generation analogy. Then, potential flow from a

source at the bottom of the vessel would give

$$\frac{\partial T^*}{\partial(x/L)} \propto \frac{\partial T}{\partial x} \propto \frac{1}{w} \propto \text{area normal to flow},$$

and the temperature gradient should increase proceeding from the bottom to the middle. However, the temperature profiles shown here exhibit the opposite behavior, indicating a substantial deviation from this type flow.

The difference between the temperature profiles for the small and large copper hemispheres (Fig. 5) apparently results because the tests with the smaller hemisphere covered the region of transition from laminar to turbulent flow. The Rayleigh number for these tests ranges from 7×10^8 to 6×10^9, spanning the approximate transition Rayleigh number of 10^9. At the lower Rayleigh numbers, the T^*'s in the upper portion of the hemisphere were somewhat larger than shown in Fig. 5, while at higher Rayleigh numbers the T^* profile nearly coincides with that of the larger hemisphere, indicating that the turbulence had become nearly fully developed.

In contrast to the temperature profiles for the other vessels, the vertical cylinder profiles (Figs. 6 and 9) are linear over much of their length. This linear temperature profile (Fig. 6) suggests a flow model (similar to that adopted by Evans *et al.* [6]) consisting of a thin boundary layer at the wall and vertical slug flow of the core. Using this flow model it is possible to predict the core velocity, w_c if $\partial T^*/\partial(x/L)$ and $Nu = f(Ra)$ are known. The relationship is probably most easily understood using the internal heat generation approach, although identical results are also obtained for the quasi-steady case. As discussed previously, a heat generating fluid creates a temperature gradient in the core as it rises. In the absence of heat transfer or mixing, this temperature gradient will be linear if the core velocity is constant. Noting that

$$\frac{\partial T}{\partial x} = \frac{1}{w_c}\frac{\partial T}{\partial t} \tag{17}$$

and that

$$\rho C_p \frac{\partial T}{\partial t} = \frac{q}{V} \tag{18}$$

it can be shown [10] that the core velocity is given by

$$w_c = \frac{4(q/A)}{\rho C_p D\left(\dfrac{\partial T}{\partial x}\right)} \tag{19}$$

or if $Nu = C_1 Ra^{1/3}$, then

$$w_c = \frac{4(L/D)(q/A)^{1/4}}{\rho C_p C_2 \dfrac{\partial T^*}{\partial(x/L)}}. \tag{20}$$

For $(q/A) = 0{\cdot}1\,\text{W/cm}^2$ the resulting core velocity in these experiments is 0·5 cm/s.

The $1/D$ dependence of w_c in equation (20) is to be expected from the continuity equation since the core cross sectional area is proportional to D^2, whereas the boundary-layer area is proportional to D. The dependence, $w_c \propto L$, indicates that the volume flow rate in the core, and therefore in the boundary layer, is proportional to the cylinder length L. This result compares to

$$\text{volume flow rate} \propto L^{3/4} \tag{21}$$

for free convective laminar flow where $Nu \propto Ra^{1/4}$ [22], and to

$$\text{volume flow rate} \propto L^{1{\cdot}2} \tag{22}$$

for turbulent flow where $Nu \propto Ra^{0{\cdot}4}$, according to integral equation analysis for an isothermal, vertical flat plate [23]. The source of this $w_c \propto L$ dependence is the observed independence of $\partial T^*/\partial(x/L)$ on L. Because the cylinder height, L, was only changed by a factor of 2, a weak dependence of $\partial T^*/\partial(x/L)$ on L would go undetected.

Nusselt numbers

The general agreement between the Nusselt numbers for the various shapes (as indicated in Fig. 4) is not too surprising considering that King [24] obtained similar agreement for convection from vertical cylinders and planes, horizontal wires, spheres, and blocks. In both cases this agreement is probably due as much to the comparison of surface average heat transfer coefficients as to basic similarity in the details of the processes. For instance, Jakob [25] has shown that the average heat-transfer coefficient from a horizontal plate is nearly the same as for a vertical plate, in spite of the 2:1 variation in the average heat-transfer coefficient between the top and the bottom of the horizontal plate. Whatever the cause of the agreement, correlation of all the data by a single expression suggests that the correlation may apply to other shapes as well.

In comparing our Nusselt numbers with those in the literature, we find that quasi-steady, turbulent, free convection within enclosed vessels has been investigated neither for the cryogenic fluids studied here, nor for other fluids. Schmidt [1], reporting on transient turbulent convection ($3 \times 10^8 < Ra < 5 \times 10^{11}$) of water and alcohols within spheres, found that $Nu = 0{\cdot}119\,Ra^{1/3}$ using the average wall-to-bulk fluid temperature difference. Evans and Stefany [2] use the expression $Nu = 0{\cdot}55\,Ra^{1/4}$ to fit their transient laminar ($6 \times 10^5 < Ra < 7 \times 10^9$) experiments of free convection of water, glycerine, etc., within horizontal and vertical cylinders. Both the Schmidt and the Evans and Stefany results are in close agreement with the expressions recommended by Jakob [24] (based on King's data):

$$Nu = 0{\cdot}555\,Ra^{1/4} \tag{23}$$

for laminar flow, and

$$Nu = 0{\cdot}129\,Ra^{1/3} \tag{24}$$

for turbulent natural convection outside horizontal and vertical cylinders, vertical planes, blocks, and spheres. In contrast, we obtain

$$Nu = 0{\cdot}166\,Ra^{1/3} \tag{25}$$

when fitting the LD_2 and LN_2 data with the exponent fixed at 1/3.

Because of the different fluids used and the different mode of heat transfer (quasi-steady instead of transient) this positive 27 per cent deviation of our results from the classical Jakob expression is not entirely unexpected. In fact, Deaver and Eckert [4] also observed a substantial positive deviation (28 per cent at $Ra = 10^6$) from the Jakob expression for their quasi-steady laminar experiments with water and ethylene glycol in horizontal cylinders ($3 \times 10^3 < Ra < 10^7$). Thus enhanced heat transfer may be a characteristic of quasi-steady natural convection.

SUMMARY AND CONCLUSIONS

The goal of this study was to provide heat-transfer design data for liquid hydrogen and deuterium moderators and targets which are used in high energy physics experiments. Because internal heat generation is difficult to achieve in the laboratory, we simulate the internal heat generation with a quasi-steady cooling process. Thus, quasi-steady natural convection of LD_2, LH_2, and LN_2 within a sphere, hemisphere, horizontal cylinder, and vertical cylinder has been studied experimentally for the case of a nearly uniform wall temperature. From this study we conclude:

1. A single expression,

$$Nu = 0{\cdot}104\, Ra^{0{\cdot}352}$$

correlates the LN_2 and LD_2 data over the range $7 \times 10^8 < Ra < 6 \times 10^{11}$ with a standard deviation of 10 per cent, whereas the hydrogen Nusselt numbers are 8 per cent lower. In all cases the thermal properties listed in Table 2 should be used in applying the correlation, since it was developed using these property values. In applying this correlation to other fluids, an additional systematic error of 10 per cent could result because of the uncertainty in the thermal properties (principally in the thermal conductivity) of liquid deuterium.

2. An enhancement of heat transfer may be characteristic of *quasi-steady* free convection within enclosures because the Nusselt numbers for both these results and those of Deaver and Eckert [4] exceed the Nusselt numbers typical of *transient* convection within enclosures by about 27 per cent.

3. The temperature field within the vessels is characterized by the virtual absence of horizontal temperature gradients—except for a thin boundary layer at the wall. For fully developed turbulent flow the dimensionless vertical temperature profile is independent of Rayleigh number for a given vessel shape. The temperature profiles for the sphere, hemisphere, and horizontal cylinder are nearly identical (Fig. 5), while the S profile for the vertical cylinders (Fig. 6) is independent of L/D for $L/D = 2$ and 4.

4. The effect of wall resistance is small. Hemispheres having a significant wall resistance (greater wall temperature gradient) exhibited only a small reduction in the Nusselt number compared to the low wall resistance hemispheres. The temperature profile is almost unchanged.

Finally, correlation of the Nusselt numbers for the variety of shapes tested here by a single expression, suggests that this correlation may apply to other shapes as well, provided they have a modest aspect ratio. Further evidence in support of the possibly greater generality of the results is the existence of a nearly universal vertical temperature profile for vessels with both end and side wall cooling (spheres, hemispheres and horizontal cylinders).

Acknowledgements—A number of people in the Cryogenics Division contributed to the successful completion of this study. In particular I wish to thank: R. O. Voth and C. F. Sindt, who aided in the design of the apparatus; L. M. Anderson, who built and helped operate the apparatus; and W. J. Hall who wrote the data reduction programs.

This work was performed under the auspices of the U.S. Energy Research and Development Administration, and their support is gratefully acknowledged.

REFERENCES

1. E. Schmidt, Versuche zum Wärmeübergang bei natürlicher Konvection, *Chem. Ing. Tech.* **28**, 175–180 (1956).
2. L. B. Evans and N. E. Stefany, An experimental study of transient heat transfer to liquids in cylindrical enclosures, *Chem. Engng Prog. Symp. Ser.* **62**, No. 64, 209–215 (1966).
3. H. G. Maahs, Transient natural convection heat transfer in a horizontal cylinder, Ph.D. dissertation, Chem. Library, U. of Wash. (1964).
4. F. K. Deaver and E. R. G. Eckert, An interferomatic investigation of convective heat transfer in a horizontal fluid cylinder with wall temperature increasing at a uniform rate, in *Heat Transfer* 1970 (Proc. 4th Int. Heat Transfer Conf., Paris–Versailles 1970), Vol. 4. Elsevier, Amsterdam (1970).
5. J. A. Clark, A review of pressurization, stratification, and interfacial phenomena, in *International Advances in Cryogenic Engineering*, edited by K. D. Timmerhaus, Sections M–U, pp. 259–283. Plenum Press, New York (1965).
6. L. B. Evans, R. C. Reid and E. M. Drake, Transient natural convection in a vertical cylinder, *A.I.Ch.E. Jl* **14**, 251–259 (1968).
7. R. G. Schwind and G. C. Vliet, Observations and Interpretations of Natural Convection and Stratification in Vessels, *Proc. of the 1964 Heat Transfer and Fluid Mechanics Institute*, edited by W. H. Giedt and S. Levy, pp. 51–68. Stanford University Press, Stanford, Calif. (1964).
8. J. W. Tatom and W. O. Carlson, Transient turbulent free convection in closed containers, in *Proc. 3rd Int. Heat Transfer Conf., Chicago*, Vol. 2, pp. 163–171. A.I.Ch.E., New York (1966).
9. H. Z. Barakat and J. A. Clark, Analytical and experimental study of the transient laminar natural convection flows in partially filled liquid containers, *Proc. 3rd Int. Heat Transfer Conf., Chicago*, Vol. 2, pp. 152–162. A.I.Ch.E., New York (1966).
10. D. E. Daney, Turbulent natural convection of liquid deuterium, hydrogen, and nitrogen within enclosed vessels, Nat. Bur. Stand. (U.S.) I.R. Report 75-807.
11. R. Prydz, The thermodynamic properties of deuterium, Nat. Bur. Stand. (U.S.) Report 9276 (April 1967).
12. J. P. Brouwer, A. M. Vossepoel, C. J. N. Van Den Meijdenberg and J. J. M. Beenakker, Specific heat of the liquid mixtures of neon and hydrogen isotopes in the phase separation region—II. The system Ne–D_2, *Physica, s' Grav.* **50**, 125–148 (1970).
13. E. C. Kerr, E. B. Rifkin, H. L. Johnson and J. T. Clarke, Condensed gas calorimetry—II. Heat capacity of ortho-

deuterium between 13·1 and 23·6 K melting and boiling points, heats of fusion and vaporization. Vapor pressure of liquid ortho-deuterium, *J. Am. Chem. Soc.* **73**, 282–284 (1951).
14. V. G. Konareva and N. S. Rudenko, Measurements of the viscosity of hydrogen isotopes along the curve of liquid–vapor equilibrium, *Zh. Fiz. Khim.* **41**(9), 2387–2388 (1967).
15. H. M. Roder, G. E. Childs, R. D. McCarty and P. E. Angerhofer, Survey of the properties of the hydrogen isotopes below their critical temperatures, Nat. Bur. Stand. (U.S.) Tech. Note 641 (August 1973).
16. H. M. Roder, L. A. Weber and R. D. Goodwin, Thermodynamic and related properties of parahydrogen from the triple point to 100°K at pressures to 340 atm, Nat. Bur. Stand. (U.S.) Monogr. 94 (August 1965).
17. R. D. McCarty and L. A. Weber, Thermophysical properties of parahydrogen from the freezing liquid line to 5000 R for pressures to 10 000 psia, Nat. Bur. Stand. (U.S.) Tech. Note 617 (April 1972).
18. T. R. Strobridge, The thermodynamic properties of nitrogen from 64 to 300°K between 0·1 and 200 atm, Nat. Bur. Stand. (U.S.), Tech. Note 129 (January 1962).
19. H. J. M. Hanley, R. D. McCarty and W. M. Haynes, The viscosity and thermal conductivity coefficients for dense gaseous liquid argon, krypton, xenon, nitrogen and oxygen, *J. Phys. Chem. Ref. Data* **3**(9), 979–1018 (1974).
20. R. W. Powers, R. W. Mattox and H. L. Johnston, Thermal conductivity of condensed gases—II. The thermal conductivities of liquid normal and of liquid parahydrogen from 15 to 27°K, *J. Am. Chem. Soc.* **76**, 5972–5973 (1954).
21. H. M. Roder and D. E. Diller, Thermal conductivity of gaseous and liquid hydrogen, *J. Chem. Phys.* **52**(11), 5928–5949 (1970).
22. W. M. Rohsenow and H. Y. Choi, *Heat, Mass, and Momentum Transfer*, p. 162. Prentice-Hall, Englewood Cliffs, NJ (1961).
23. W. M. Rohsenow and H. Y. Choi, *Heat, Mass, and Momentum Transfer*, p. 204. Prentice-Hall, Englewood Cliffs, NJ (1961).
24. M. Jakob, *Heat Transfer*, Vol. 1, p. 530. John Wiley, New York (1959).
25. M. Jakob, *Heat Transfer*, Vol. 1, p. 532. John Wiley, New York (1959).

CONVECTION NATURELLE TURBULENTE DU DEUTERIUM DE L'HYDROGENE ET DE L'AZOTE LIQUIDES DANS UN RECIPIENT CLOS

Résumé—On á étudié expérimentalement la convection naturelle quasi-stationnaire du deutérium, de l'hydrogène et de l'azote liquides à l'intérieur d'une sphère, d'un hémisphère, d'un cylindre horizontal et d'un cylindre vertical, dans le cas d'une température pariétale presque uniforme. Une expression unique reliant les nombres de Nusselt et de Rayleigh,

$$Nu = 0{,}104\,Ra^{0{,}352}$$

rend compte des données relatives au deutérium et à l'azote dans le domaine $7.10^8 < Ra < 6.10^{11}$, tandis que les nombres de Nusselt pour l'hydrogène sont de 8 pour cent inférieurs. Le champ de température dans les récipients ne présente pratiquement pas de gradient horizontal. Un seul profil de température adimensionnel caractérise la distribution verticale de température pour chaque forme d'enceinte, les profils pour la sphère, l'hémisphère et le cylindre horizontal étant presque identiques.

TURBULENTE NATÜRLICHE KONVEKTION IN FLÜSSIGEM DEUTERIUM, WASSERSTOFF UND STICKSTOFF IN GESCHLOSSENEN BEHÄLTERN

Zusammenfassung—Quasi-stationäre natürliche Konvektion von flüssigem Deuterium, Wasserstoff und Sauerstoff in einer Kugel, Halbkugel, einem waagerechten und senkrechten Zylinder wurde experimentell untersucht für den Fall, nahezu einheitlicher Wandtemperatur. Eine einzige Korrelation von Nusselt und Rayleigh–Zahlen

$$Nu = 0{,}104\,Ra^{0{,}352}$$

entspricht den Versuchswerten von Deuterium und Stickstoff im Bereich von $7 \times 10^8 < Ra < 6 \times 10^{11}$ während die Nusselt–Zahlen für Wasserstoff 8% tiefer liegen. Das Temperaturfeld in den Behältern weist im wesentlichen keine horizontalen Temperaturgradienten auf. Ein einziges dimensionsloses Temperaturprofil charakterisiert die senkrechte Temperaturverteilung für jede Behälterform, wobei die Profile für die Kugel, die Halbkugel und den waagerechten Zylinder nahezu identisch sind.

ТУРБУЛЕНТНАЯ ЕСТЕСТВЕННАЯ КОНВЕКЦИЯ ЖИДКОГО ДЕЙТЕРИЯ, ВОДОРОДА И АЗОТА В ЗАМКНУТЫХ СОСУДАХ

Аннотация — Квази-стационарная естественная конвекция жидкого дейтерия, водорода и азота внутри сферы, полусферы, горизонтального цилиндра и вертикального цилиндра изучалась экспериментально для случая почти однородной температуры стенки. Единственное выражение, связывающее числа Нуссельта и Релея,

$$Nu = 0{,}104 Ra^{0{,}352}$$

обобщает данные по тейтерию и азоту в диапазоне $7 \times 10^8 < Ra < 6 \times 10^{11}$, в то время как значения критерия Нуссельта для водорода на 8% ниже. Температурное поле внутри сосудов практически свободно от горизонтальных температурных градиентов. Единственный безразмерный температурный профиль характеризует вертикальное распределение температуры для каждой формы сосуда, причем профили для шара, полусферы и горизонтального цилиндра почти идентичны.